iScience

CellPress
OPEN ACCESS

Article

Information integration for decision-making in desert locusts

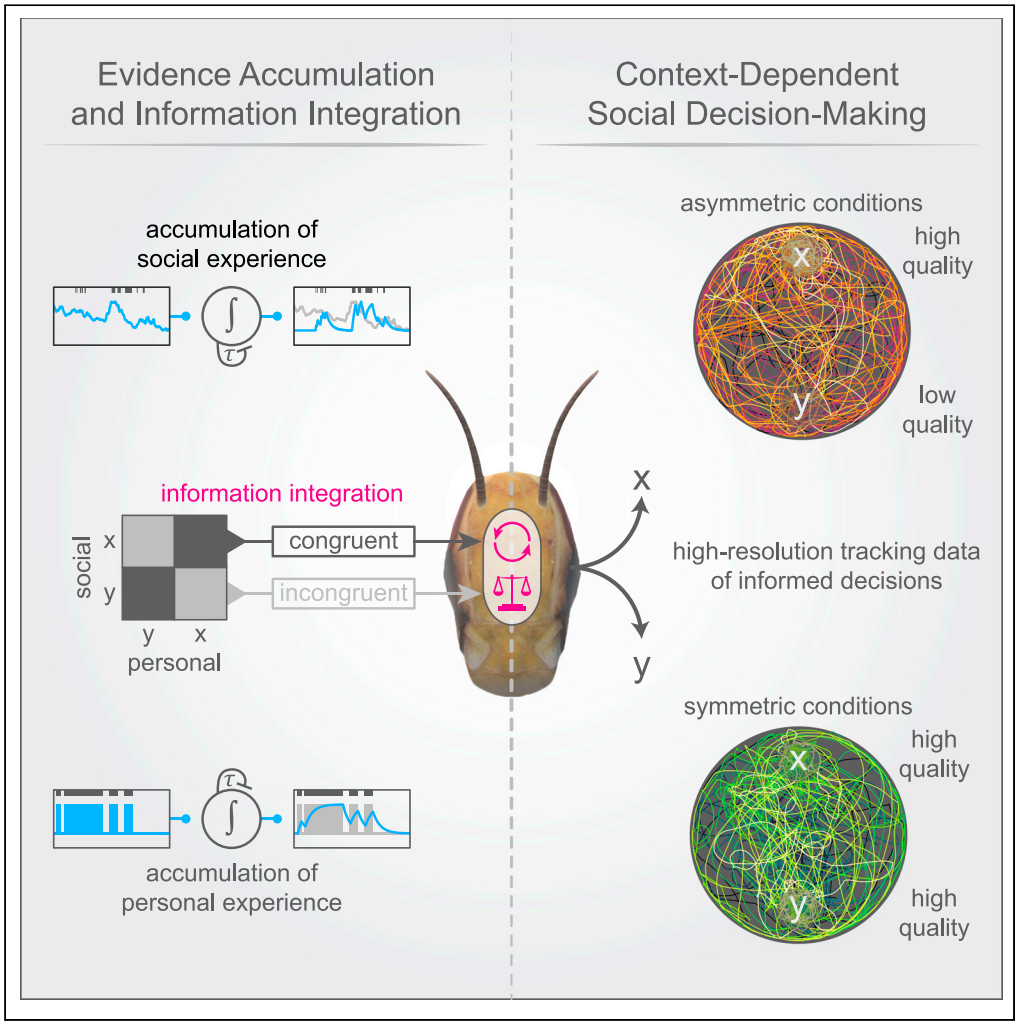

Yannick Günzel, Felix B. Oberhauser, Einat Couzin-Fuchs

einat.couzin@uni-konstanz.de

Highlights

Locust patch choice is strongly influenced by the social context

Foraging locusts select the best available patch, but split when options are equal

We infer the locust decision-making rule guiding patch choice

Locusts integrate private with social information for informed decision-making

Günzel et al., iScience 26, 106388
April 21, 2023 https://doi.org/10.1016/j.isci.2023.106388

iScience

CellPress
OPEN ACCESS

Article

Information integration for decision-making in desert locusts

Yannick Günzel,[1,2,3,4] Felix B. Oberhauser,[3,4] and Einat Couzin-Fuchs[2,3,4,5,*]

SUMMARY

Locust swarms can extend over hundred kilometers, and starvation compels this ancient pest to devour everything in its path. Theory suggests that gregarious behavior benefits foraging efficiency, yet the role of social cohesion remains elusive. To this end, we collected high-resolution trajectories of individual and grouped gregarious desert locusts in a 2-choice assay with patches of either similar or different quality. Carefully maintaining animals' identities allowed us to monitor each individual's experience and estimate the leaky accumulation process of personally acquired and socially derived evidence. We fitted data to a Bayesian model to gain insight into the decision-making system for patch selection. By disentangling the relative contribution of each information class, our study suggests that locusts balance incongruent evidence but reinforce congruent ones. We provide insight into the collective foraging decisions of social (but non-eusocial) insects and present locusts as a powerful empirical system to study individual choices and consequent collective dynamics.

INTRODUCTION

The migratory desert locust (*Schistocerca gregaria*) can form swarms spanning several hundred square kilometers and, driven by starvation, can devour everything on its path through semi-arid environments with fragmented vegetation structures.[1,2] Usually, locust bands form in arid recession areas when favorable weather conditions allow the development of green vegetation.[3,4] With increasing locust densities at sparse food patches, social cues—like the resulting mechanical stimulation between animals—initiate gregarisation of previously solitarious animals.[5–7] This density-dependent phase polyphenism (reviewed by M.P. Pener and S.J. Simpson[8], D.A. Cullen et al.[9], and S.J. Simpson[10]), throughout which animals transition from avoiding others to approaching them, causes a devastating autocatalytic chain reaction of aggregation that promotes further aggregation and, consequently, local population growth.[11,12] Unlike solitarious locusts, which populate recession areas in low densities and forage alone, gregarious locusts march together[2,13,14,15] and—upon depletion of local resources—invade new regions. Nevertheless, despite this ancient plague's vast humanitarian, ecological, and economic impact,[16] little is known about how locusts utilize different sources of information to guide their devastating foraging campaigns.

The transition from solitary to group foraging also implies significant differences in the type, quality, and quantity of information animals can gather. Generally, information can be obtained through direct interactions with the environment—"private information"; or derived from the behavior of others—"social information".[17–19] Consequently, solitarious locusts are likely limited to private information, while social information is abundant in swarms. Integrating both information classes, when available, could allow individuals to update their self-obtained "beliefs" with those of surrounding conspecifics. This information integration may be essential in high-population densities where nutritional unpredictability is increased and environmental cues for locating potential resources are limited.[20] Various phase-dependent morphological and physiological changes accompany the transition from a sedentary solitarious foraging strategy with a restricted host-plant range[21,8] to nutritionally opportunistic group foraging. Notably, a reallocation of growth investment from low-level sensory areas (*e.g.*, primary olfactory neuropils) to higher processing ones (*e.g.*, central complex) during the transition from the solitarious to the gregarious phase[22] may reflect a shift in environmental complexity, and consequently, the need for increased information processing.

Group-living individuals routinely utilize information produced intentionally or unintentionally by others, and often simple rules can explain how social information is used in the underlying decision system.[23–26]

[1]International Max Planck Research School for Quantitative Behaviour, Ecology and Evolution from Lab to Field, 78464 Konstanz, Germany

[2]Department of Biology, University of Konstanz, 78464 Konstanz, Germany

[3]Department of Collective Behavior, Max Planck Institute of Animal Behavior, 78464 Konstanz, Germany

[4]Centre for the Advanced Study of Collective Behaviour, University of Konstanz, 78464 Konstanz, Germany

[5]Lead contact

*Correspondence: einat.couzin@uni-konstanz.de

https://doi.org/10.1016/j.isci.2023.106388

In eusocial insects, foraging is facilitated by sophisticated communication and recruitment signals, such as the waggle dance in bees[27] or pheromone trails in ants.[28] In other species, the transfer of social information relies on inadvertent cues provided by the behavior of others.[17,18] For example, gregarious insects such as cockroaches and fruit flies collectively select resource patches without active recruitment[29,30] via the effect of retention: animals stay longer when more conspecifics are present.[29,31–33] The presence of others can indicate both resource location and quality, offering discrete and graded information, respectively.[18] This often results in consensus formation through a collective quorum decision on a single option. Cockroach groups, for instance, collectively select a single shelter out of two equal options.[33] Notably, however, social information can be outdated or noisy, and in many cases, animals may favor using private information when available.[34] Moreover, the presence of others at a resource patch may also indicate partial exploitation/depletion, competition, or—as observed by Bazazi et al.[35]—potential danger through cannibalism. Consequently, in some cases, the social context can even result in a preference inversion.[31,36] Therefore, optimal foraging decisions rely on integrating information from both classes according to their reliability and availability.[37]

Optimization processes for integrating different types of information are commonly utilized in multi-modal sensory integration during navigation.[38–40] The core premise—gaining higher estimation accuracy through merging information classes, weighted by their uncertainty—can also be valid for private and social information sources and has been successfully applied to human decisions.[24,41] To our knowledge, empirical animal studies have rarely used similar frameworks for integrating private and social information, potentially due to difficulties in quantifying the accumulation of evidence in each information class.

To this end, we investigate how accumulated personal experience and the availability of social cues impact locust foraging decisions in symmetric and asymmetric environments. For this, we investigated the locust decision system by extending a Bayesian estimation for social decision-making by Arganda et al.[25] to also capture each animal's previous decisions. We test how the social context impacts patch choice and whether locusts form a consensus when two options are available. For this, we tracked the behavior of locust groups varying in size during simple patch choice assays of either equal or different quality. Our study shows that locusts use both private and social information, which they optimally update by balancing incongruent (opposing) cues and reinforcing congruent (aligned) ones.

RESULTS

Condition-dependent formation of consensus

We studied locust foraging dynamics in a simple behavioral assay in which gregarious locusts were tested in different group sizes (N = 1, 5, 10, 15, 30 animals) against two patch options (Figure 1A, Video S1) of either equal symmetric (*EQ*-trials) or unequal asymmetric (*UE*-trials) quality (Figure 1B i). We tracked animals while retaining accurate labels of individual identity for 30 min to estimate (history-dependent) interactions among conspecifics and with the patches (Figure 1Bii). Throughout the trials, animals explored the arena with multiple visits to both patches per animal (Figure S1A) with visit times that reflected the asymmetry in patch quality (Figures S1B and S1C). As locust behavior is strongly density-dependent, we estimated animal density profiles across the entire arena to characterize each animal's social experience within, around, and outside the patches at any given time (Figure 1C and mov. 4).

Within a few minutes, animal density at the patches increased (Figure 2A). The density at the patches was higher than the maximum density observed in two control regions (Figure 1Bi, dotted circles). Notably, we observed this in both conditions (*EQ*, Figure 2Aii; *UE*, Figure 2Aiv), both patch types (*HQ* and *LQ*), and all group sizes (see Table S1 for p values and *s*-values). Further, animal density was consistently higher at the high-quality (*HQ*) patch in *UE*-trials (Figure 2Aiii–iv), but similar for both *HQ*-patches in the *EQ*-trials (Figure 2Ai–ii; see Table S1 for p values, *s*-values, and effect sizes). This imbalance during *UE*-trials resulted in higher preference index values than during *EQ*-trials (Figure 2B; see Table S1 for p values, *s*-values, and effect sizes).

The clear preference exhibited in all group sizes of the *UE*-trials was also reflected by the high consensus level routinely exceeding a three-quarters super-majority (Figure 2C; purple swarm plots and time courses). Interestingly, when two *HQ* patches were present, locusts mostly split into two groups rather than forming a quorum. It is important to note that capacity-wise, there was no "hard" boundary on quorum formation even for the largest groups, as seen by the high consensus values in the *UE*-trials. The tendency to split

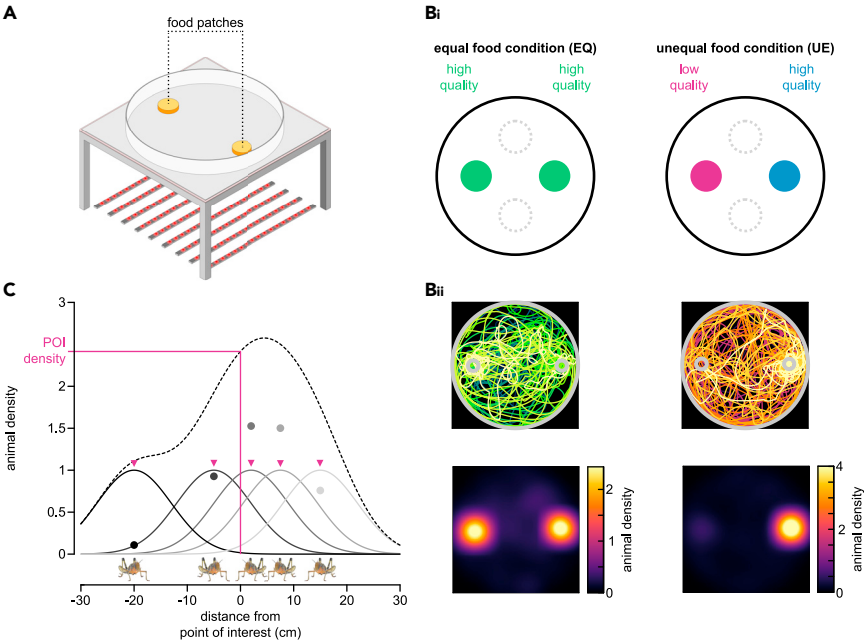

Figure 1. Experimental setup and overview of conducted analysis steps to investigate locust foraging behavior

(A) Schematic of the circular arena (d = 90 cm) used. Two food patches were placed at a randomly selected, opposing position (six possible configurations).

(B) Animals were tested under one of two conditions: An equal food condition (*EQ*, left), with two high-quality patches, or an unequal one (*UE*, right), containing one high-quality patch and a low-quality one. As a control, we compared the aggregation at patches with empty regions (dotted circles). Animals were visually tracked using marker-less multi-animal tracking software that reliably maintained individuals' identities throughout the trial (Bii, first row, example trajectories for a trial with N = 10 animals, color codes animals' IDs). Trajectories were rotated such that food patches were aligned horizontally, with the high-quality patch on the right for *UE*-experiments. Local animal density was estimated based on individual trajectories (Bii, second row, averaged across all frames and animals for the example trial above).

(C) Densities were estimated by 2-D Gaussian filtering of individual animal positions within the arena. Shown is a 1-D example with five animals. Solid lines represent local densities induced by each animal. Dots represent local, animal-centric ("perceived") densities. The dotted line indicates the overall animal density in 1D space that could be measured at a specific point of interest (POI) as, for instance, the center of a patch.

during *EQ*-trials increases with group size (Figure 2C; green swarm plots), suggesting patch choices were driven not only by positive social cohesion (explaining the high degree of consensus when only a few animals were at the patches, *e.g.* for N < 15 and at the beginning of all trails) but also by other factors, such as perceived patch values or competition avoidance.

Presence of others dictates individual patch interactions

To further dissect the individual factors governing the observed dynamics, we investigated how locust density (social cohesion) impacts patch choice decisions under different conditions. Tracking individual animals while maintaining their identities throughout the trials allowed us to evaluate how the prevailing animal density affected the probabilities of joining and staying at a patch. Overall, regardless of the patch quality, we found that animals joined patches faster (Figure 3A) and stayed longer (Figure 3B) when local density was high. Nevertheless, the resulting consensus maps were markedly different between *EQ*- and *UE*-trials, also when evaluated against local animal densities at the patches (Figure 3C). With larger differences in consensus values between the *EQ*- and *UE*-trials for more crowded patches, we examined whether the positive social feedback is inverted when crowding is high (which would indicate explicit competition avoidance). However, this was not the case, as locusts almost always preferred the more populated patch in both *EQ*- and *UE*-trials (Figure 3D). The preference for the more populated option was even more apparent when choices were evaluated against the difference in densities between the two options, showing a higher preference toward the more populated option for almost the entire range (except for density differences of less than 1, when patches were nearly equally populated; Figure 3E). Taken together,

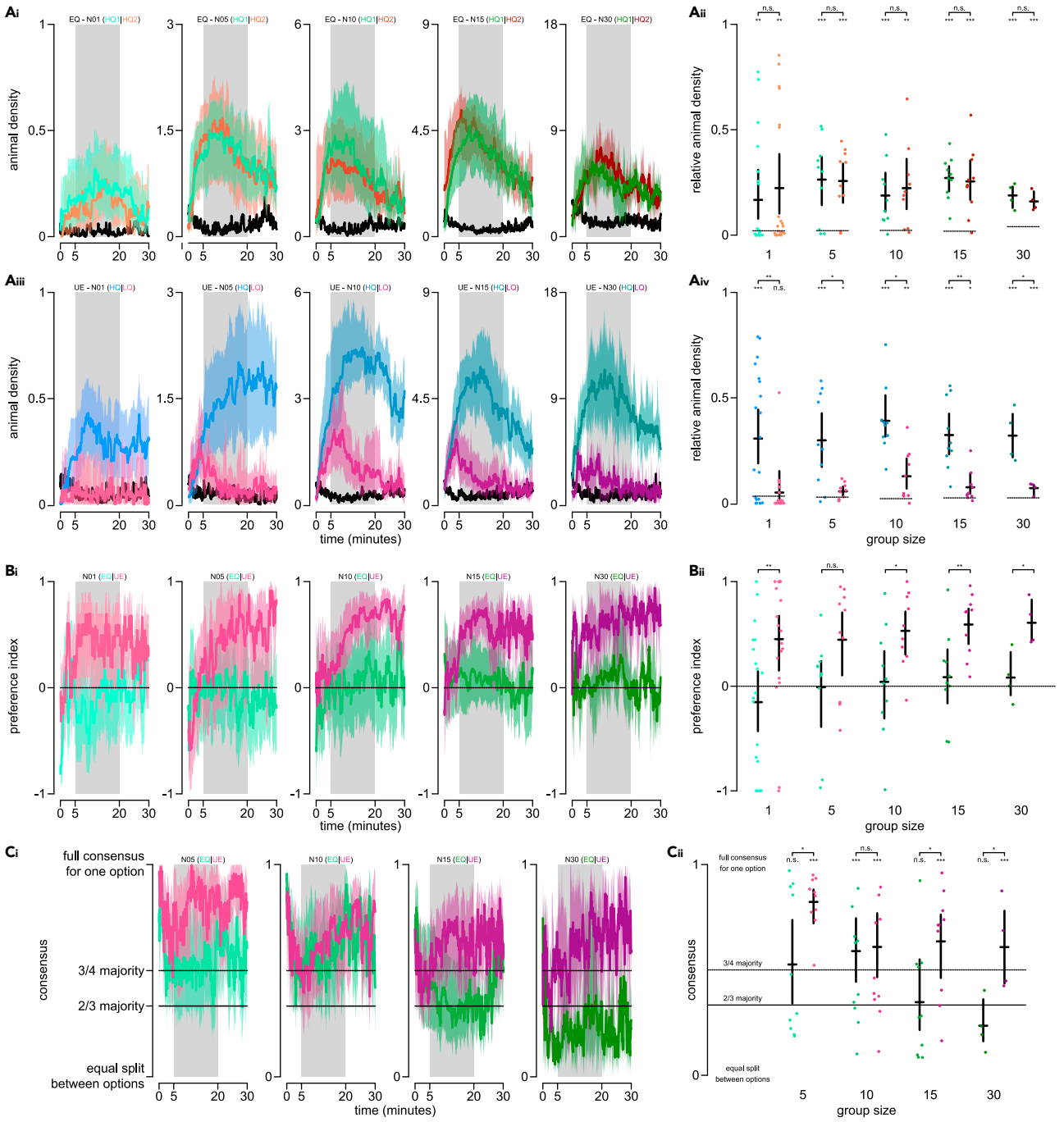

Figure 2. Temporal dynamics of animal densities at patches, preference development, and consensus formation

(A) Animal density time courses (Ai, Aiii) and averages (Aii, Aiv) for the equal (*EQ*; shades of green/red; Ai–ii) and unequal (*UE*; shades of blue/magenta; Aiii–iv) patch conditions, separated by group size. Colored time courses show animal density at the respective patches, while black lines show the maximum animal density in the control regions (see Figure 1Bi, dashed circles). The instantaneous maximum density in control regions was used as baseline in Aii and Aiv (bottom lines).

(B) Preference index time courses (Bi) and averages (Bii) for the equal (*EQ*; shades of green) and unequal (*UE*; shades of purple) patch conditions, separated by group size. The stronger the values differ from zero (dotted line), the stronger the preference toward one patch over the other. For *UE*-trials, positive values indicate a stronger preference for the high-quality option.

(C) Consensus time courses (Ci) and averages (Cii) for the equal (*EQ*; shades of green) and unequal (*UE*; shades of purple) patch conditions, separated by group size. A value of zero indicates equal animal density at both patches, while a value of one shows full consensus—all animals are at a single patch. Black solid lines indicate the degree of consensus that would result from a two-thirds super-majority, while the dotted black lines refer to a three-quarters

Figure 2. *Continued*

super-majority, respectively. For time courses (Ai, Aiii, Bi, and Ci), solid colored lines represent grand means across animals and trials, while shaded colored areas indicate 95% confidence intervals around the mean. For averages (Aii, Aiv, Bii, and Cii), each trial's time course was averaged between minutes five and 20 (majority of patch selection events; gray areas in time course panels). Crosses indicate the position of the mean (horizontal) and corresponding 95% confidence intervals (vertical). Individual points indicate trial means. Not significant: n.s.; $p < 0.05$: *; $p < 0.01$: **; $p < 0.001$: ***; see Table S1 for p values, s-values, and effect sizes.

the density-dependent joining behavior exhibited in both patch conditions suggests that the presence of others serves as an inadvertent social cue, which conveys discrete (location) information but is insufficient for graded (quality) information. Since such information can be directly acquired by sampling the patches during feeding events (accumulation of private information), we continued to investigate how the two information channels interact during the patch selection process.

Locusts integrate private with social information for efficient foraging

Information about the location and quality of patches forms the basis of foraging decisions. We dissected these decision-making processes by modeling personal and social evidence accumulation (Figure 4Ai) and their interactions (Figures 4Aii and Aiii). A Bayesian formalism illustrates that locust decisions can be well estimated from balanced differences of accumulated within-class evidence (Table S3; k_q and k_s are both larger than zero but smaller than one) and by employing an optimal integration of different information classes (private and social information).

Across group sizes and both patch conditions, individual information classes estimated the animal's patch choice well above chance level (gray distributions; Figure 4C). Generally, estimations based on social information alone outperformed those solely based on directly acquired private information and resulted in the smallest AICc values (apart from *EQ*-trials with groups of five animals). Above all, the integration of both information classes under either patch condition (*EQ* or *UE*) significantly exceeds the single cue probabilities of correct estimations (colored swarm plots; Figure 4C). The spread of all decision events, pooled across all conditions, located according to their individual channel predictors and color-coded by the value of their integrated estimate (Figure 4B) further corroborates this. Here, a simple average across all decisions would estimate worse in 81.90% of the *EQ*- and 78.95% of the *UE*-trials.

Personally acquired and socially derived evidence can be congruent, *i.e.*, both estimating correctly ($P > 0.5$, upper right [orange] quarter in Figures 4Aii and 4D) or incorrectly ($P < 0.5$, bottom left corners); or they can be incongruent with one correct and one incorrect estimation (blue quarters in Figure 4Aii). When evidence is incongruent, there is a conflict regarding the information on which to base a decision. The decision rule used here provides an intermediate estimate in these cases, based on the certainty levels of both channels (top-left and bottom-right in Figure 4D). This estimate was generally better than a simple average with a significant rescue in performance ($P_{integration} > 0.5$ where either $P_{pers.}$ or $P_{soc.} < 0.5$; Figure 4E). For *EQ*-trials, when $P_{EQ,pers.} < 0.5$, then $P_{integration} > 0.5$ in 72.01% of the cases. Likewise, when $P_{EQ,soc.} < 0.5$, then $P_{integration} > 0.5$ in 65.32% of the cases. The same held true for *UE*-trials. When $P_{UE,pers.} < 0.5$, then $P_{integration} > 0.5$ in 70.20% of the cases, and when $P_{UE,soc.} < 0.5$, then $P_{integration} > 0.5$ in 66.00% of the cases. The same integration rule with congruent evidence (both information classes estimating the same outcome) results in reinforcement uncertainty reduction, producing an estimate which is more extreme than both single cues. Since most cases of congruent evidence are correct (less likely that both information classes are wrong), this resulted in more correct answers for both patch conditions ($P_{integration} > 0.5$; *EQ* : 88.19%; *UE* : 81.36%; Figure 4E). Taken together, inferring the locust decision-making rule used in patch choice suggests that animals balance incongruent and reinforce congruent information. This reflects an effective integration of the two information classes, which form stronger "opinions" when evidence aligns as well as consider the respective strengths of the single cues in case of conflicting evidence.

DISCUSSION

This study provides a framework for studying collective decision-making based on evidence accumulation in different information classes. We show that locusts collectively select the best available food but split into two groups when both options are equal. Our data suggest that these fission-fusion dynamics originate from discrete information on the location of food conveyed by the retention of others. However, by estimating the relative evidence provided by either class of information, private or social, we show that

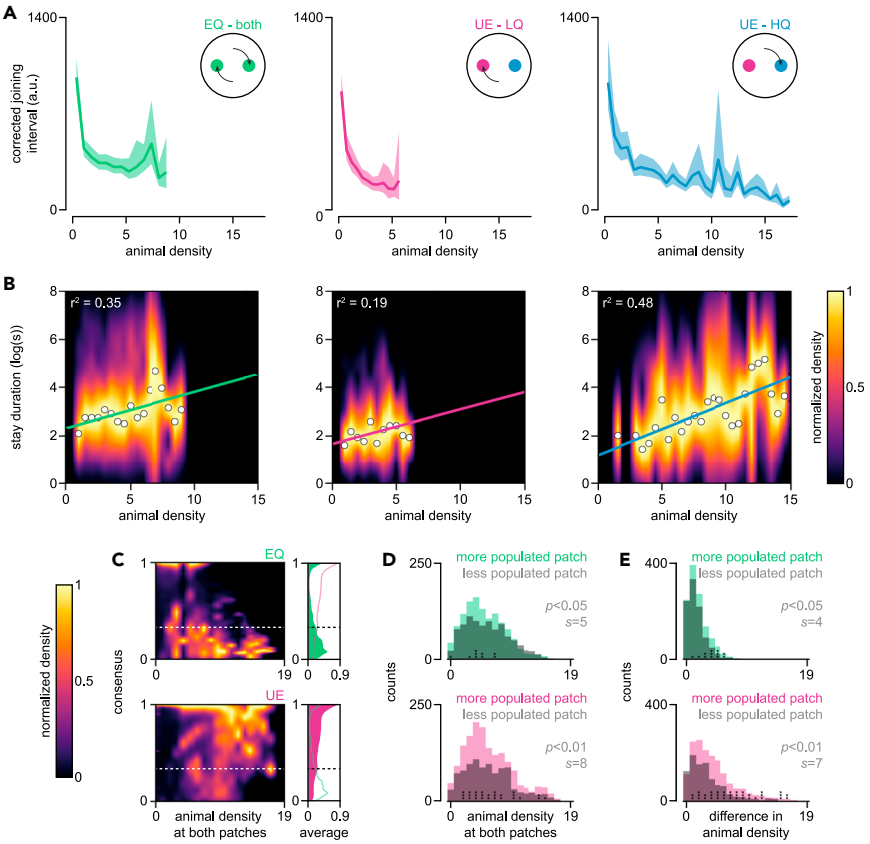

Figure 3. Prevailing animal densities shape individual and collective decisions

(A) Interval between two consecutive joining events as a function of the average prevailing animal density during the interval. Solid lines represent grand means across animals, trials, and group sizes (N = 5, 10, 15, 30 animals; averages per group size can be found in Figure S1E). Shaded areas indicate corresponding 95% confidence intervals. For the equal, high-quality, (*EQ*) condition (left panel), data for both patches were pooled, while for the unequal-quality (*UE*) condition, the low-quality (*LQ*, center panel) and the high-quality (*HQ*, right panel) patches were analyzed separately. Joining intervals were corrected for the number of remaining animals to account for a "depletion" of available animals.

(B) Bivariate density contour plots show the duration of individual visits to a patch as a function of the average prevailing animal density during the stay. Columns were min-max normalized, and white superimposed dots indicate the location of the maximum of the respective column. Maxima were used to fit a linear model to the data (colored line). For the equal, high-quality, (*EQ*) condition (left panel), data for both patches were pooled, while for the unequal-quality (*UE*) condition, the low-quality (*LQ*, center panel) and the high-quality (*HQ*, right panel) patches were analyzed separately. (C) Bivariate density contour plots showing how the degree of consensus changes as a function of the animal density summed over both patches (*EQ* top row; *UE* bottom row). Columns were min-max normalized. Superimposed dotted white lines indicate the location of a two-thirds super-majority. Average consensus values per row are shown on the right. Data were pooled across all group sizes (N = 5, 10, 15, 30 animals).

(D) Histograms comparing the number of events a new animal joined the more populated patch (colored bars) or the less populated one (gray bars) for different animal densities summed over both patches (*EQ* top row; *UE* bottom row).

(E) Histograms showing under which difference in animal density a new animal either joined the more (colored bars) or the less (gray bars) populated option (*EQ* top row; *UE* bottom row). We tested whether the difference in counts in D and E was significantly different from zero using paired two-sample, two-tailed bootstrap randomization tests (see p values and *s*-values in the respective panels). Further, we applied two-tailed binomial tests with a proposed probability of joining the more populated patch of 0.5 to each bin (see Table S2 for p values and *s*-values).

locusts balance incongruent evidence based on their respective strength. At the same time, they reinforce congruent information to form stronger opinions when evidence aligns.

Reliable sensory-motor decisions rely on stochastic processes to sample information from noisy environments,[19] to integrate evidence from different senses[40] according to the internal state,[13,42,43] and ultimately to generate an appropriate context-dependent motor output.[44] Integration can occur at different scales: from the dendritic

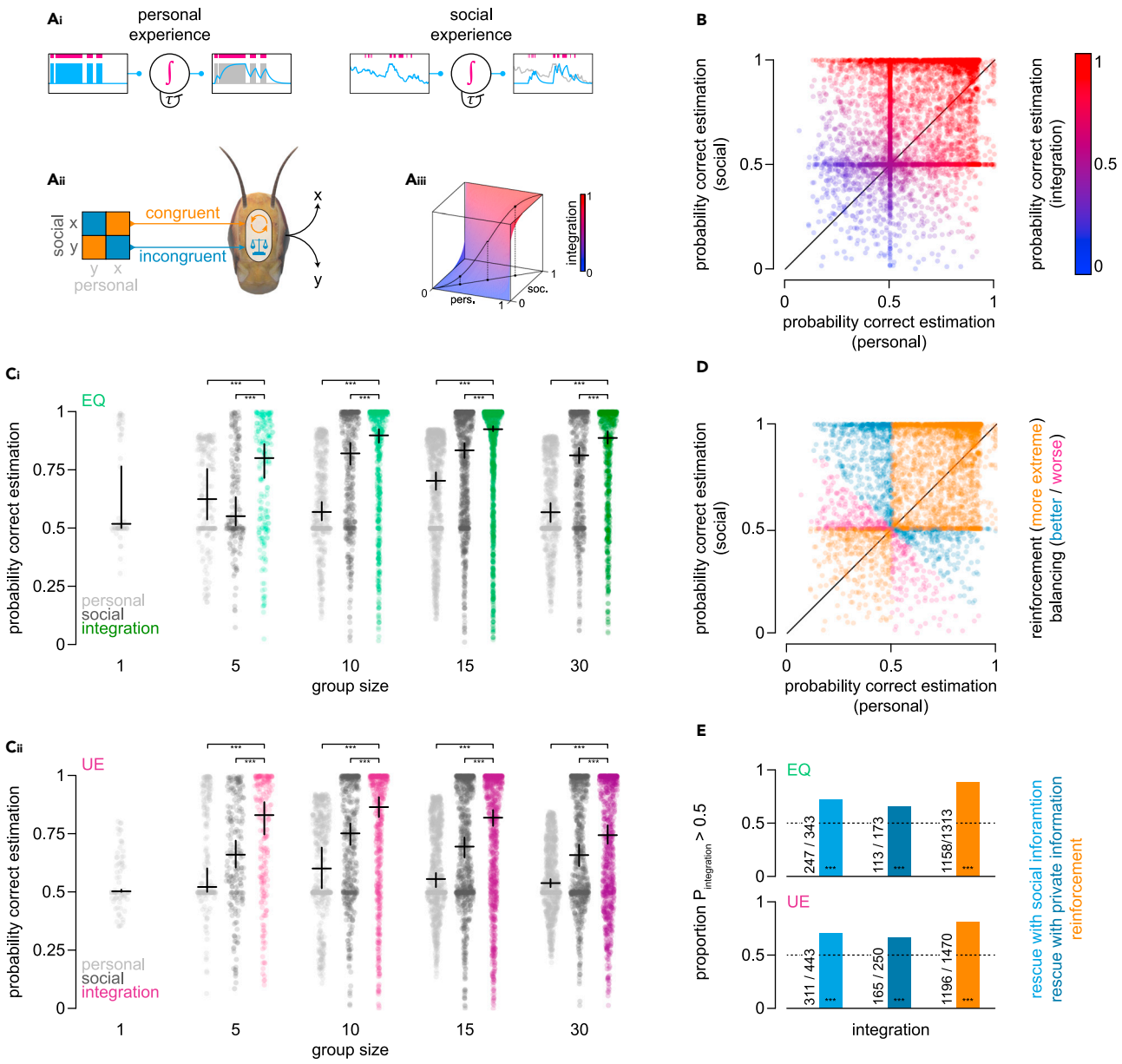

Figure 4. Inference of the locust decision-making rule used in patch choice

(A) Illustration showing the concept of evidence accumulation (Ai), the Bayesian integration of private and social information (Aii), and the integration rule (Aiii). Our model for estimating patch choices is based on the leaky accumulation of both personal and social experiences over time (Ai; accumulation bouts indicated in red). We assumed that the accumulation of private information occurred during patch selection bouts and the accumulation of social information during reorientation (pausing) bouts. Accumulated evidence in each information class (private, social) contributed to the estimation of the next choice, *i.e.*, to join patch *x* or *y* (Aii). If both information classes estimated the same choice, information was congruent (orange quarters). However, if estimations were conflicted, information was incongruent (blue quarters). An emerging property of our model was that congruent information got reinforced in the integration process, while incongruent information got balanced (Aiii).

(B) Scatterplot showing the distribution of patch choices estimated based on private information alone (abscissa), social information alone (ordinate), and color-coded by their resultant integration estimate.

(C) Swarm plots showing the probability distributions of correct patch estimation based on private information (light gray), social information (dark gray), and the integration of the two classes (color). Data for the equal patch condition (*EQ*) are in the upper row in shades of green for the integration, while the unequal patch condition (*UE*) is below with shades of magenta for the integration. Corrected Akaike information criterion values are listed in Table S5. Crosses indicate sample medians (horizontal) and corresponding 95% confidence intervals (vertical). Statistical analysis was done using paired two-sample, two-tailed bootstrap randomization tests with Bonferroni correction (see Table S6 for p values, s-values, and effect sizes).

Figure 4. *Continued*

(D) Same as in B but with color indicating whether the probability of a correct estimation was more extreme than either of the underlying information classes, indicating reinforcement (orange); or whether the integration resembled a weighted average, indicating balancing (blue: better estimation than a simple average, magenta: worse than a simple average).

(E) Proportion of when the probability for a correct patch choice estimation following the integration of private and social information was above 0.5, separated by whether the underlying evidence was congruent (orange bars, indicating reinforcement) or incongruent (blue bars, indicating balancing). Light blue bars show how strong socially derived information ($P_{soc.} > 0.5$) could rescue ($P_{integration} > 0.5$) weak personally acquired information ($P_{pers.} < 0.5$). Dark blue bars show how strong personally acquired information ($P_{pers.} > 0.5$) could rescue ($P_{integration} > 0.5$) weak socially derived information ($P_{soc.} < 0.5$). Orange bars pool reinforcement of weak information ($P_{soc.} < 0.5$ and $P_{pers.} < 0.5$) or strong information ($P_{soc.} > 0.5$ and $P_{pers.} > 0.5$). Underlying counts are noted on the side. Statistical analysis was done using two-tailed binomial tests against a value of 0.5 (see Table S6 for p values and s-values). Not significant: n.s.; $p < 0.05$: *; $p < 0.01$: **; $p < 0.001$: ***.

integration of signals arriving at a single neuron,[45,46] over small pooling networks of several cells,[47] up to whole brain regions.[48] Here, we followed the principles of a drift-diffusion model, a standard model for perceptual decision-making strategies reviewed by R. Ratcliff et al., 2016,[49] by assuming a leaky accumulation of evidence for the location of food (Figure 4). We based the accumulation processes on private and social information, which resemble higher-order constructs of different modalities. Social information in locusts is likely based on vision, but auditory, haptic, and olfactory cues may also contribute. For simplicity, we consolidated the different aspects of this multi-modal construct into one term, "animal density" (Figures 1C, 2A, and 3). Moreover, models solely based on social information explained most of the variation (AICc values in Table S5) with high reliability values (parameter *s* in Table S3). Both corroborate the strong impact of the social context on patch choice (Figure 3), reflecting how aggregation promotes further aggregation in locusts,[11,12] reviewed by M.P. Pener and S.J. Simpson, 2009.[8] On the other hand, private information about a patch's quality is most likely to be gustatory. Estimation accuracy solely based on private information (Figure 4C) exceeding chance level suggests that animals could remember and discriminate the location of a "good" food patch from that of a "bad" one. This indicates that locusts can accumulate private evidence for several items, store it over seconds, and retrieve the information effectively. Future experiments may elucidate the relative contribution of different modalities and the mechanisms underlying their accumulation processes.

When assessing an event's likelihood, subjective knowledge and objective facts about such likelihoods are indistinguishable for the observer. Subjective confidence for the occurrence of a given event can be described in terms of Bayesian probabilities, which represent the degree of an observer's belief,[25,50] reviewed by.[51] Different classes of information can be combined to increase confidence while making a decision, often according to their inherent uncertainty levels.[52] Information integration processes can explain elevated performance levels in insect navigation and foraging,[38–40,53,54] human perception,[55] and collective decision-making.[41] Here, we show that a Bayesian formalism can also reliably estimate foraging decisions by integrating different information classes (Figure 4), consistently resulting in significantly better estimations following the integration of private with social information than for an individual information class alone (Figure 4C). We projected decisions according to their respective social and personal evidence to gain more insight into the decision rule and why it outperforms each information class. By dividing the 2-D "evidence space" into congruent (Figures 4Aii and 4D, orange quarter and points, respectively) and incongruent (Figure 4Aii blue quarter; Figure 4D blue and magenta points), we derive that providing a certainty context allows for integrating both information classes effectively. The social decision-making rule rescues performance by balancing evidence in incongruent cases (blue bars in Figure 4E) while increasing estimation confidence when evidence agrees (orange bars in Figure 4E).

The collective dynamics we observed of locust groups splitting between equal high-quality patches differ from observations on other gregarious insect species.[33,56] Analyzing consensus formation across time and group size revealed that positive social cohesion, which was driving instances of consensus in relatively small groups during *EQ*-trials (Figure 3C, N = 5), breaks with an increasing number of animals (Figure 3C, N > 5) and the acquisition of private information over time. Future studies may investigate the relative contribution of different information classes under different conditions across different temporal and spatial foraging scales.

Predicting locust behavior is crucial for taking preventive measures against future outbreaks and applying directed control efforts against existing ones. To date, however, forecasts of swarms and marching bands' locations still fall short of precision.[57] Quantitative approaches have been largely insightful for generating testable predictions about the gregarisation process,[58,59] swarm movement,[60,61] and foraging.[62] However, large-scale empirical studies to corroborate them remain scarce (but not[6,63] for long-term recordings of

gregarisation experiments). By utilizing a simple foraging assay, in which the personal and social experiences of all individuals are monitored across time, our study provides an empirical confirmation for the prediction that gregarious behavior can improve foraging success in locusts[59] and shows this behavior to be dynamically amended by personal experience.

The basic framework for evaluating decision processes based on private and social information could be combined with agent-based modeling to disentangle the contribution of interrelated factors and make testable predictions about how this scales with size (social and spatial) and time. The extreme polyphenism of locusts and the fast continuous transition between the gregarious and solitarious phase additionally allows tuning of the valence of social parameters.[8] With the high-resolution mapping of personal experience, nutritional state, and behavior, locust foraging offers a powerful empirical system to investigate local individual decisions and their resulting collective dynamics.

Limitations of the study

Our study suggests a framework to analyze evidence accumulation and social decision-making, which we apply to infer the decision rules used in patch choice under two simple experimental conditions. However, due to the nature of the experiments and inter-connectivity between private and social information here (*i.e.*, acquiring private information by sampling a patch also increases the density of animals at that patch), we were not able to equally scan the private-social parameter space (long-tailed distributions following the integration (Figure 4C); few combinations of high-personal and low-social values (Figure 4B)). Future experimental manipulations could target the more conflicting regions of parameter space (*e.g.*, by combining naive and experienced or hungry and starved individuals). This could also be expanded further using other scenarios with more gradual differences in patch qualities and/or larger environments with multiple options to investigate the validity of the results reported across contexts. Furthermore, the current study does not differentiate actual patch selection bouts from "simply being around" a patch (*i.e.*, when the animal's centroid is in close vicinity to the patch). Although we show that patch weight loss increases with increasing cumulative animal density (Figure S1D), we cannot completely rule out the occurrence of animals watching others feed instead of feeding themselves.

STAR★METHODS

Detailed methods are provided in the online version of this paper and include the following:

- KEY RESOURCES TABLE
- RESOURCE AVAILABILITY
  - Lead contact
  - Materials availability
  - Data and code availability
- EXPERIMENTAL MODEL AND SUBJECT DETAILS
- METHOD DETAILS
  - Experimental setup
  - Experimental procedure
  - Preparation of patches
- QUANTIFICATION AND STATISTICAL ANALYSIS
  - Visual tracking of animals
  - Data analysis
  - Inferring the locust decision-making rule used in patch choice
  - Integration of private and social information for patch choice
  - Statistical analysis

SUPPLEMENTAL INFORMATION

Supplemental information can be found online at https://doi.org/10.1016/j.isci.2023.106388.

ACKNOWLEDGMENTS

The authors thank J. Gübel, Y. Hertenberger, J. Roller, and M. Spagnuolo for help during data collection, A. Land for help tracking animals, and the two anonymous reviewers for detailed and helpful feedback. This work was completed with the support of the Deutsche Forschungsgemeinschaft (DFG, German Research Foundation) under Germany's Excellence Strategy—EXC 2117–422037984.

DECLARATION OF INTERESTS

Authors declare that they have no competing interests.

INCLUSION AND DIVERSITY

We support inclusive, diverse, and equitable conduct of research.

Received: September 7, 2022
Revised: December 3, 2022
Accepted: March 8, 2023
Published: March 13, 2023

REFERENCES

1. Kennedy, J.S. (2009). The behaviour of the desert locust (schistocerca gregaria (forsk.))(orthopt.) in an outbreak centre. Trans. R. Entomol. Soc. Lond. *89*, 385–542.

2. Ellis, P.E., and Ashall, C. (1957). Field studies on diurnal behaviour, movement and aggregation in the desert locust (schistocerca gregaria forskål).

3. Tucker, C.J., Hielkema, J.U., and Roffey, J. (1985). The potential of satellite remote sensing of ecological conditions for survey and forecasting desert-locust activity. Int. J. Rem. Sens. *6*, 127–138.

4. Keith, C. (2016). Desert Locust. *Biological and Environmental Hazards, Risks, and Disasters*, pp. 87–105.

5. Leo Lester, R., Grach, C., Paul Pener, M., and Simpson, S.J. (2005). Stimuli inducing gregarious colouration and behaviour in nymphs of schistocerca gregaria. J. Insect Physiol. *51*, 737–747.

6. Despland, E., and Simpson, S.J. (2000). The role of food distribution and nutritional quality in behavioural phase change in the desert locust. Anim. Behav. *59*, 643–652.

7. Simpson, S.J., Despland, E., Hägele, B.F., and Dodgson, T. (2001). Gregarious behavior in desert locusts is evoked by touching their back legs. Proc. Natl. Acad. Sci. USA *98*, 3895–3897.

8. Paul Pener, M., and Simpson, S.J. (2009). Locust phase polyphenism: an update. Adv. Insect Physiol *36*, 1–272.

9. Cullen, D.A., Cease, A.J., Latchininsky, A.V., Ayali, A., Berry, K., Buhl, J., De Keyser, R., Foquet, B., Hadrich, J.C., Matheson, T., et al. (2017). From molecules to management: mechanisms and consequences of locust phase polyphenism. Adv. Insect Physiol *53*, 167–285. Elsevier.

10. Simpson, S.J. (2022). A journey towards an integrated understanding of behavioural phase change in locusts. J. Insect Physiol. *138*, 104370.

11. Roessingh, P., and Simpson, S.J. (1994). The time-course of behavioural phase change in nymphs of the desert locust, schistocerca gregaria. Physiol. Entomol. *19*, 191–197.

12. Simpson, S.J., McCAFFERY, A.R., and Hägele, B.F. (2007). A behavioural analysis of phase change in the desert locust. Biol. Rev. *74*, 461–480.

13. Bazazi, S., Romanczuk, P., Thomas, S., Schimansky-Geier, L., Hale, J.J., Miller, G.A., Sword, G.A., Simpson, S.J., and Couzin, I.D. (2011). Nutritional state and collective motion: from individuals to mass migration. Proc. Biol. Sci. *278*, 356–363.

14. Buhl, J., Sumpter, D.J.T., Couzin, I.D., Hale, J.J., Despland, E., Miller, E.R., and Simpson, S.J. (2006). From disorder to order in marching locusts. Science *312*, 1402–1406.

15. Ariel, G., and Ayali, A. (2015). Locust collective motion and its modeling. PLoS Comput. Biol. *11*, e1004522.

16. Steedman, A., et al. (1988). Locust Handbook.

17. Danchin, E., Giraldeau, L.A., Valone, T.J., and Wagner, R.H. (2004). Public information: from nosy neighbors to cultural evolution. Science *305*, 487–491.

18. Dall, S.R.X., Giraldeau, L.A., Olsson, O., McNamara, J.M., and Stephens, D.W. (2005). Information and its use by animals in evolutionary ecology. Trends Ecol. Evol. *20*, 187–193.

19. Davidson, J.D., and El Hady, A. (2019). Foraging as an evidence accumulation process. PLoS Comput. Biol. *15*, e1007060.

20. Despland, E., and Simpson, S.J. (2005). Food choices of solitarious and gregarious locusts reflect cryptic and aposematic antipredator strategies. Anim. Behav. *69*, 471–479.

21. Despland, E. (2005). Diet breadth and anti-predator strategies in desert locusts and other orthopterans. J. Orthoptera Res. *14* (2), 227–233.

22. Ott, S.R., and Rogers, S.M. (2010). Gregarious desert locusts have substantially larger brains with altered proportions compared with the solitarious phase. Proc. Biol. Sci. *277*, 3087–3096.

23. Aplin, L.M., Farine, D.R., Mann, R.P., and Sheldon, B.C. (2014). Individual-level personality influences social foraging and collective behaviour in wild birds. Proc. Biol. Sci. *281*, 20141016.

24. Miller, N., Garnier, S., Hartnett, A.T., and Couzin, I.D. (2013). Both information and social cohesion determine collective decisions in animal groups. Proc. Natl. Acad. Sci. USA *110*, 5263–5268.

25. Arganda, S., Pérez-Escudero, A., and de Polavieja, G.G. (2012). A common rule for decision making in animal collectives across species. Proc. Natl. Acad. Sci. USA *109*, 20508–20513.

26. Couzin, I.D., Krause, J., Franks, N.R., and Levin, S.A. (2005). Effective leadership and decision-making in animal groups on the move. Nature *433*, 513–516.

27. von Frisch, K., et al. (1967). Dance Language and Orientation of Bees.

28. Czaczkes, T.J., Grüter, C., and Ratnieks, F.L.W. (2015). Trail pheromones: an integrative view of their role in social insect colony organization. Annu. Rev. Entomol. *60*, 581–599.

29. Lihoreau, M., Deneubourg, J.-L., and Rivault, C. (2010). Collective foraging decision in a gregarious insect. Behav. Ecol. Sociobiol. *64*, 1577–1587.

30. Lihoreau, M., Clarke, I.M., Buhl, J., Sumpter, D.J.T., and Simpson, S.J. (2016). Collective selection of food patches in drosophila. J. Exp. Biol. *219*, 668–675.

31. Günzel, Y., McCollum, J., Paoli, M., Galizia, C.G., Petelski, I., and Couzin-Fuchs, E. (2021). Social modulation of individual preferences in cockroaches. iScience *24*, 101964.

32. Calvo Martín, M., Eeckhout, M., Deneubourg, J.-L., and Nicolis, S.C. (2021). Consensus driven by a minority in heterogenous groups of the cockroach periplaneta americana. iScience *24*, 102723.

33. Amé, J.M., Halloy, J., Rivault, C., Detrain, C., and Deneubourg, J.L. (2006). Collegial decision making based on social amplification leads to optimal group formation. Proc. Natl. Acad. Sci. USA *103*, 5835–5840.

34. Grüter, C., and Leadbeater, E. (2014). Insights from insects about adaptive social information use. Trends Ecol. Evol. *29*, 177–184.

35. Bazazi, S., Buhl, J., Hale, J.J., Anstey, M.L., Sword, G.A., Simpson, S.J., and Couzin, I.D. (2008). Collective motion and cannibalism in locust migratory bands. Curr. Biol. *18*, 735–739.

36. Laurent Salazar, M.O., Nicolis, S.C., Calvo Martín, M., Sempo, G., Deneubourg, J.L., Planas-Sitjà, I., and Planas-Sitjà, I. (2017). Group choices seemingly at odds with individual preferences. R. Soc. Open Sci. *4*, 170232.

37. Dunlap, A.S., Nielsen, M.E., Dornhaus, A., and Papaj, D.R. (2016). Foraging bumble bees weigh the reliability of personal and social information. Curr. Biol. *26*, 1195–1199.

38. Hoinville, T., and Wehner, R. (2018). Optimal multiguidance integration in insect navigation. Proc. Natl. Acad. Sci. USA *115*, 2824–2829.

39. Dacke, M., Bell, A.T.A., Foster, J.J., Baird, E.J., Strube-Bloss, M.F., Byrne, M.J., and El Jundi, B. (2019). Multimodal cue integration in the dung beetle compass. Proc. Natl. Acad. Sci. USA *116*, 14248–14253.

40. Buehlmann, C., Mangan, M., and Graham, P. (2020). Multimodal interactions in insect navigation. Anim. Cognit. *23*, 1129–1141.

41. Park, S.A., Goïame, S., O'Connor, D.A., and Dreher, J.-C. (2017). Integration of individual and social information for decision-making in groups of different sizes. PLoS Biol. *15*, e2001958.

42. Vogt, K., Zimmerman, D.M., Schlichting, M., Hernandez-Nunez, L., Qin, S., Malacon, K., Rosbash, M., Pehlevan, C., Cardona, A., and Samuel, A.D.T. (2021). Internal state configures olfactory behavior and early sensory processing in drosophila larvae. Sci. Adv. *7*, eabd6900.

43. Sareen, P.F., McCurdy, L.Y., and Nitabach, M.N. (2021). A neuronal ensemble encoding adaptive choice during sensory conflict in drosophila. Nat. Commun. *12*, 4131–4213.

44. Ache, J.M., Namiki, S., Lee, A., Branson, K., and Card, G.M. (2019). State-dependent decoupling of sensory and motor circuits underlies behavioral flexibility in drosophila. Nat. Neurosci. *22*, 1132–1139.

45. DasGupta, S., Ferreira, C.H., and Miesenböck, G. (2014). Foxp influences the speed and accuracy of a perceptual decision in drosophila. Science *344*, 901–904.

46. Groschner, L.N., Chan Wah Hak, L., Bogacz, R., DasGupta, S., and Miesenböck, G. (2018). Dendritic integration of sensory evidence in perceptual decision-making. Cell *173*, 894–905.e13.

47. Borst, A., and Bahde, S. (1988). Visual information processing in the fly's landing system. J. Comp. Physiol. *163*, 167–173.

48. Bahl, A., and Engert, F. (2020). Neural circuits for evidence accumulation and decision making in larval zebrafish. Nat. Neurosci. *23*, 94–102.

49. Ratcliff, R., Smith, P.L., Brown, S.D., and McKoon, G. (2016). Diffusion decision model: current issues and history. Trends Cognit. Sci. *20*, 260–281.

50. Pérez-Escudero, A., and de Polavieja, G. (2011). Collective animal behavior from bayesian estimation and probability matching. Nat. Prec. 1.

51. Meyniel, F., Sigman, M., and Mainen, Z.F. (2015). Confidence as bayesian probability: from neural origins to behavior. Neuron *88*, 78–92.

52. Cheng, K., Shettleworth, S.J., Huttenlocher, J., and Rieser, J.J. (2007). Bayesian integration of spatial information. Psychol. Bull. *133*, 625–637.

53. Legge, E.L.G., Wystrach, A., Spetch, M.L., and Cheng, K. (2014). Combining sky and earth: desert ants (melophorus bagoti) show weighted integration of celestial and terrestrial cues. J. Exp. Biol. *217*, 4159–4166.

54. Wystrach, A., Mangan, M., and Webb, B. (2015). Optimal cue integration in ants. Proc. Biol. Sci. *282*, 20151484.

55. Ernst, M.O., and Banks, M.S. (2002). Humans integrate visual and haptic information in a statistically optimal fashion. Nature *415*, 429–433.

56. Jeanson, R., Deneubourg, J.-L., Grimal, A., and Theraulaz, G. (2004). Modulation of individual behavior and collective decision-making during aggregation site selection by the ant messor barbarus. Behav. Ecol. Sociobiol. *55*, 388–394.

57. Sword, G.A., Lecoq, M., and Simpson, S.J. (2010). Phase polyphenism and preventative locust management. J. Insect Physiol. *56*, 949–957.

58. Collett, M., Despland, E., Simpson, S.J., and Krakauer, D.C. (1998). Spatial scales of desert locust gregarization. Proc. Natl. Acad. Sci. USA *95*, 13052–13055.

59. Georgiou, F., Buhl, J., Green, J.E.F., Lamichhane, B., and Thamwattana, N. (2021). Modelling locust foraging: how and why food affects group formation. PLoS Comput. Biol. *17*, e1008353.

60. Topaz, C.M., Bernoff, A.J., Logan, S., and Toolson, W. (2008). A model for rolling swarms of locusts. Eur. Phys. J. Spec. Top. *157*, 93–109.

61. Bernoff, A.J., Culshaw-Maurer, M., Everett, R.A., Hohn, M.E., Strickland, W.C., and Weinburd, J. (2020). Agent-based and continuous models of hopper bands for the australian plague locust: how resource consumption mediates pulse formation and geometry. PLoS Comput. Biol. *16*, e1007820.

62. Lihoreau, M., Charleston, M.A., Senior, A.M., Clissold, F.J., Raubenheimer, D., Simpson, S.J., and Buhl, J. (2017). Collective foraging in spatially complex nutritional environments. Philos. Trans. R. Soc. Lond. B Biol. Sci. *372*, 20160238.

63. Despland, E., and Simpson, S.J. (2000). Small-scale vegetation patterns in the parental environment influence the phase state of hatchlings of the desert locust. Physiol. Entomol. *25*, 74–81.

64. Walter, T., and Couzin, I.D. (2021). Trex, a fast multi-animal tracking system with markerless identification, and 2d estimation of posture and visual fields. Elife *10*, e64000.

65. Bazazi, S., Bartumeus, F., Hale, J.J., and Couzin, I.D. (2012). Intermittent motion in desert locusts: behavioural complexity in simple environments. PLoS Comput. Biol. *8*, e1002498.

66. Ariel, G., Ophir, Y., Levi, S., Ben-Jacob, E., and Ayali, A. (2014). Individual pause-and-go motion is instrumental to the formation and maintenance of swarms of marching locust nymphs. PLoS One *9*, e101636.

67. Akaike, H. (1973). Information Theory and an Extension of the Maximum Likelihood Principle (Springer), p. 199.

68. Akaike, H. (1974). A new look at the statistical model identification. IEEE Trans. Automat. Control *19*, 716–723.

69. Hurvich, C.M., and Tsai, C.-L. (1993). A corrected akaike information criterion for vector autoregressive model selection. J. Time Ser. Anal. *14*, 271–279.

70. MacKinnon, J.G. (2009). Bootstrap hypothesis testing. Handbook of computational econometrics *183*, 213.

71. Wasserstein, R.L., Schirm, A.L., and Lazar, N.A. (2019). Moving to a World beyond "P_s 0.05".

72. Nelson, M. (2022). mybinomtest. https://www.mathworks.com/matlabcentral/fileexchange/24813-mybinomtest-s-n-p-sided.

STAR★METHODS

KEY RESOURCES TABLE

REAGENT or RESOURCE	SOURCE	IDENTIFIER
Deposited data	this paper	https://doi.org/10.5281/zenodo.7541780
Software and algorithms		
Analysis code	this paper	https://doi.org/10.5281/zenodo.7541780
Automated tracking	this paper	github.com/YannickGuenzel/BlobMaster3000

RESOURCE AVAILABILITY

Lead contact

Further information and requests should be directed to and will be fulfilled by the lead contact, Einat Couzin-Fuchs (einat.couzin@uni-konstanz.de).

Materials availability

This study did not generate new unique reagents.

Data and code availability

- Processed animal trajectories have been deposited at Zenodo and are publicly available as of the date of publication. The URL is: https://doi.org/10.5281/zenodo.7541780.
- Data were analyzed and plotted using custom-written MATLAB scripts. Analysis code is available at https://doi.org/10.5281/zenodo.7541780. Custom-written graphical user interface (GUI) for manually supervised tracking is available at https://github.com/YannickGuenzel/BlobMaster3000.
- Any additional information required to reanalyze the data reported in this paper is available from the lead contact upon request.

EXPERIMENTAL MODEL AND SUBJECT DETAILS

We conducted experiments with late-instar (4th, 5th larval stage) gregarious *Schistocerca gregaria* (Forskål, 1775) desert locusts. The animals were commercially obtained from a local insect breeder (b.t.b.e. Insektenzucht GmbH, Bad Wörishofen, Germany) at least one week prior to experiments. During this time, animals were kept in the experimental room under crowded conditions (approx. 200 animals per 50 × 50 × 70 cm cage) with fresh blackberry leaves *ad libitum*. Two nights before the experiments, animals were deprived of food and water to increase their foraging motivation.

METHOD DETAILS

Experimental setup

The setup consisted of a circular polyvinyl chloride (PVC) arena (d = 90 cm) with a transparent Plexiglas plate covering the top (Figure 1, inspired by Günzel et al.[31]). We prevented animals from climbing by applying petroleum jelly (Balea Vaseline, dm-drogerie markt GmbH + Co. KG, Karlsruhe, Germany) to the arena wall. Each trial lasted 30 minutes and was recorded with a single Basler camera (25 fps; acA2040 - 90μm; Basler AG, Ahrensburg, Germany) placed above the arena and equipped with an infra red (IR) long-pass filter. A custom-made infrared LED (850 nm wavelength) grid and a diffuser plate placed below the arena ensured uniform illumination for the video recordings. An additional light source (Hakutatz light emitting diode (LED) ring light, 33cm 35W Bi-color 3200-5600K) illuminated the arena from above. A white paper wall (height: 75 cm) was additionally placed around the arena to prevent animals from visual guidance or disruption throughout the trial. We kept the temperature constant (24 °C - 26 °C) during experiments and cleaned the arena with ethanol and water after each trial.

Experimental procedure

Gregarious locusts were tested individually or in groups (N = 5, 10, 15 or 30 animals) in one of two experimental conditions: equal trials (" *EQ*-trials"), in which two equal, high-quality (" *HQ*-patch") patches were placed in the arena, and unequal trials (" *UE*-trials") with one nutritious patch (*HQ*-patch, same quality as in *EQ*-trials) and one of a low nutritional value (" *LQ*-patch"). Food patches (diameter: 7.12 ± 0.40 cm, mean ± std) were placed within the arena on opposite sides (180° and 61.65 ± 1.33 cm, mean ± std apart) in one out of six possible positions (*e.g.*, positions 60° and 240° in mov. 4). Under each condition, *EQ* and *UE*, we conducted 20 trials with N = 1 animal, ten trials for each N = 5, 10, and 15 animals, and four trials with N= 30 animals. Thus, 880 animals were tested in total.

Preparation of patches

For *HQ*-patches, we mixed 500 mL tap water with 38 g gelatin from porcine skin (gel strength 300, Type A, G2500, Sigma-Aldrich, Merck KGaA, Darmstadt, Germany), 25 g honey (Gut & Günstig Bienenhonig flüssig, Edeka Zentrale Stiftung & Co. KG, Hamburg, Germany), and 25 g egg (yolk and albumen stirred beforehand; EDEKA Bio Eier, Edeka Zentrale Stiftung & Co. KG, Hamburg, Germany). In contrast, for a clear difference in quality, the *LQ*-patches consisted of 525 mL tap water and 60 g gelatine only. During the preparation, special care was taken that ingredients mix without caking. Besides the quality difference, the patches were similar in shape and size and sufficient for the entire tested group of locusts to aggregate on and around a single patch.

QUANTIFICATION AND STATISTICAL ANALYSIS

Visual tracking of animals

We obtained trajectories of individual locusts using the multi-animal tracking software TRex[64] with a critical focus on maintaining animal identities over time. For videos with densely clustered animals that were particularly difficult to track, we used a custom-written GUI in MATLAB (R2021a, The MathWorks Inc, Natick, MA, USA) that allows for manual supervision. Obtained trajectories were smoothed by convolution with a Gaussian kernel (half-width = 2 s, $\sigma = \frac{2}{3}$ s) and rotated to align the patch positions across trials (with the *HQ*-patch in *UE*-trials always on the right). Smoothing trajectories resulted in more accurate speed profiles that we used to determine walking and standing bouts. If an animal stayed for more than 5 s within the range of one body length (4 cm) around the edge of the patch, we considered this interval a 'patch selection bout' (see Figure S1D for a quantification). This minimum retention time, along with a minimum inter-bout interval of 5 s, accounted for animals just passing by or for noise in tracking, respectively.

Data analysis

We estimated local animal density by a frame-wise application of a 2-D Gaussian smoothing kernel to each animal's x/y-coordinates within the arena. We used a standard deviation that reflected the density-independent interaction range employed by locusts of approx. 7 cm.[14] We estimated the overall animal density at a given point of interest (POI) as the sum of local densities imposed by each animal in the arena (see Figure 1 and Video S1).

We used the prevailing animal density at two control regions (Figure 1Bi, dotted circles) to rule out potential aggregation outside the patches. The control regions correspond to the two patches' positions, only rotated by 90 degrees. We only considered the maximum density across the two control regions to achieve a conservative measure.

In order to determine the animals' patch preference, we calculated a preference index based on the local animal densities D (see Figure 2A) at both patches X and Y for each point in time t. Specifically, we divided the difference between animal densities by their sum ($PI_X(t) = \frac{D_X(t) - D_Y(t)}{D_X(t) + D_Y(t)}$; see Figure 2B). Thus, the stronger the preference index differs from zero, the stronger the preference toward a patch. For *UE*-trials, we subtracted the density at the *LQ*-patch from the density at the *HQ*-patch. Thus, positive values reflect a stronger preference for the *HQ*-option and negative values for the *LQ*-option.

We were interested in both whether and how animals deal with competition at crowded patches and to what degree competition affects consensus formation. For this, we estimated the degree of consensus as the absolute value of the preference index (see Figure 2C). Further, for each experimental condition (*EQ*- and *UE*-trials), we pooled data from all group sizes and binned values according to the amount of

prevailing animal density summed across both patches. We min-max normalized each column and depicted the 2-D binning as heat maps, plotted as filled contour plots without isolines (see Figure 3C).

To further investigate how the social context affects individual choices, we estimated how joining and staying at a patch is associated with animal density at the respective patch (see Figure 3). Joining intervals, *i.e.*, the interval between two consecutive joining events, were plotted against the average animal density during this interval. To account for changes in the availability of animals outside the patches, we corrected intervals during which many animals were available by multiplying each interval with the density outside the patches. Similarly, we plotted stay duration against the average animal density throughout the visit. Here, we binned stay duration and animal density as a bivariate density estimate with min-max normalized columns to reveal the respective distributions, and to test for a potential interaction between the two. For the latter, we extracted the location of the maximum density (value of one due to column-wise normalization) in each column, to which we then fitted a linear model. We used the total counts of observations per animal density column as weights to account for skewed distributions for the fit. Heat maps were depicted as filled contour plots without isolines.

Inferring the locust decision-making rule used in patch choice

We investigated the locust social decision-making system used in patch choice by adapting a previously published decision rule by Arganda et al.[25] The Bayesian estimation returns the probability of an option x being a 'good' option $P(x\ is\ good)$, given the evidence for options x and y, respectively (Equation 1). For inference of the locust decision-making rule, We fitted six parameters to our data: the reliability of private and social information (s and q, respectively), the corresponding relative impact of opposing effects between patches for each information class (k_s and k_q, respectively), and time constants for the accumulation of socially derived and personally acquired evidence (τ_s and τ_q, respectively; Equation 4. To account for the asymmetric conditions in *UE*-trials we fitted two different values for q_x and q_y, whereas $q_x = q_y$ in *EQ*-trials.

$$P(x\ is\ good|social) = \frac{1}{1+s^{-\left(N_x - k_s N_y\right)}}$$
$$P\left(x\ is\ good\middle|private\right) = \frac{1}{1+q^{-\left(E_x - k_q E_y\right)}} \quad \text{(Equation 1)}$$

Here, N_x and N_y refer to the accumulated evidence based on social information for patch x and y, respectively. Likewise, E_x and E_y refer to the accumulated evidence based on private information for patch x and y, respectively. Based on probability matching, the probability of choosing option x can be estimated ([25], Equation 2).

$$P_x = \frac{P(x\ is\ good)}{P(x\ is\ good) + P(y\ is\ good)} \quad \text{(Equation 2)}$$

Here, we extended Equation 2 for combining two information classes: private and social information (Equation 3; Figure 4Aiii).

$$P_x = \frac{P(x\ is\ good|social)P\left(x\ is\ good\middle|private\right)}{P(x\ is\ good|social)P\left(x\ is\ good\middle|private\right) + P(y\ is\ good|social)P\left(y\ is\ good\middle|private\right)} \quad \text{(Equation 3)}$$

This non-linear integration rule incorporates three aspects. First, if one information class is non-informative, the probability of choosing an option is solely based on the other information class. Second, combining congruent evidence is substantially more informative than the underlying information classes alone. Third, combining incongruent evidence accounts for the respective strengths by balancing (in contrast to averaging) both classes.

We fitted the parameters to each group size (Table S3) using Bayesian hyperparameter optimization (MATLAB built-in function *bayesopt*). The reliability of information parameters (s, q) were fitted within the upper and lower bounds of 1 and 5, respectively. This assumes an option is good when supporting evidence is substantial (*e.g.*, a patch with high animal density is more attractive). The impact of opposing effects parameters (k_q and k_s) were fitted within the upper and lower bounds of 0 and 1, respectively. Here, a value approaching one suggests that locusts choose a patch solely based on the relative difference in

accumulated evidence, whereas a value approaching zero indicates that the decision was made solely based on the absolute amount of evidence.

Following the principles of a drift-diffusion model, we modeled the accumulation of evidence as a leaky process (Equation 4) with two integrator units per information class, *i.e.*, one for each patch.

$$\tau \frac{dX(t)}{dt} = -X(t) + Y(t)$$

where:

$X(t)$: accumulated sensory variable

$Y(t)$: time − dependent personal or social context, respectively

τ : time constant for leaky accumulation

(Equation 4)

Here, the time-dependent personal context was a step function that equals 1 for frames in which the animal was feeding and 0 otherwise (see Figure 4Ai, left). The time-dependent social context was the local animal density at a patch, scaled by the focal animal's distance to the respective patch, with accumulation periods during the animal's pausing bouts outside the patches (see Figure 4Ai, right). This assumption of of social information being accumulated during pausing bouts is based on the finding that pausing bouts can be associated with reorientation maneuvers and thus potentially with decision-making processes.[65,66] Having one time constant per class of information accounts for differences in bout duration distributions (animals generally have more prolonged patch selection bouts than pausing bouts, thus accumulating private information over more extended periods than social information; Figure S1). We fitted the time constants within the upper and lower bounds of 1 second and 15 minutes, respectively.

We applied the decision rule in a discretized fashion, only at the frame right before a selection event. This means that if an animal was joining a patch at time t, the accumulated evidence for both patches and information classes one frame before were used to inform our model (private information for patches x and y: $E_x(t-1)$, $E_y(t-1)$; social information for patches x and y: $N_x(t-1)$, $N_y(t-1)$). Therefore, we only compared the animal's actual choice with a single estimation of its probability of choosing the patch, which allowed us to determine whether the estimation was correct.

Integration of private and social information for patch choice

Interested in how locusts use different information classes to make decisions, we dissected the relative contribution of private and social information in the integration process. For this, we simulated the absence of information in the respective class by setting the corresponding reliability parameter, s or q (Equation 1), to a value of one. Exemplary cases for which this would occur naturally are the absence of private information before the animal's first patch selection bout, or ambiguity in social information when other animals are distributed equally among the two options. Note, however, that this does not include fitting new parameters. Instead, we interrogated the existing model to which degree the quality of a single information class alone can correctly estimate the animal's choice and how both classes of information are being integrated. To account for an effective reduction in the number of parameters, we applied the Akaike information criterion, corrected for small sample sizes (AICc,[67–69]; Equation 5).

$$AIC_c = n\log\left(\frac{RSS}{n}\right) + 2k + \frac{2k^2 + 2k}{n - k - 1}$$

where :

n : sample size

RSS : residual sum of squares

k : 1 + number of fitted parameters

(Equation 5)

Statistical analysis

We performed all analysis steps in MATLAB. If not stated otherwise, we report averages as grand means (means of trial means within one patch condition and group size) with bootstrapped 95% confidence intervals (B = 5000 samples) as error bars or shaded areas, respectively. Statistical inference was based on

bootstrap randomization tests with $B = 5 * 10^6$ samples (*c.f.*[70]). Briefly, we applied the same statistical summary to the permutated test statistic T^* and to the test statistic of the original sample T and determined the probability p of observing T^* being the same or more extreme. Note that this approach yields a lowest achievable p-value of $1/B = 2 * 10^{-7}$.

For a two-sample, two-tailed comparison with observations z (mean $\overline{z}$, standard deviation σ_z, sample size n) and y (mean $\overline{y}$, standard deviation σ_y, sample size m), we used the test statistic noted down in Equation 6. Here, we drew bootstrap samples from a joint distribution of z and y with n samples assigned to z^* and m samples to y^*.

$$T_{two-sample} = \frac{|\overline{z} - \overline{y}|}{\sqrt{\frac{\sigma_z^2}{n} + \frac{\sigma_y^2}{m}}} \quad \text{(Equation 6)}$$

For a paired two-sample, two-tailed comparison of observations z and y with the resulting pairwise difference x (mean $\overline{x}$, standard deviation σ_x, sample size n), we used the test statistic noted down in Equation 7. Here, we drew samples from the empirical distribution $\overline{x}_i = x_i - \overline{x}$ with $i = 1, \ldots, n$.

$$T_{pairedtwo-sample} = \frac{|\overline{x}|}{\sigma_x / \sqrt{n}} \quad \text{(Equation 7)}$$

For a one-sample, two-tailed comparison with observation z (mean $\overline{z}$, sample size n) and a pre-determined value μ_0 (*e.g.* 0.5), we used the test statistic noted down in Equation 8. Here, we drew samples from the empirical distribution $\overline{z}_i = z_i - \overline{z} + \mu_0$ with $i = 1, \ldots, n$.

$$T_{one-sample} = |\overline{z} - \mu_0| \quad \text{(Equation 8)}$$

Reports of p-values are complemented with corresponding s-values (Shannon information, $s = -log_2(p)$). Shannon information is expressed in bits of information against the tested hypothesis and helps to portray evidential value better.[71] In the case of two-sample comparisons, we further provide effect sizes (Cohen's d).

To evaluate whether animals were joining the more populated patch, binned by the animal density summed across both patches (Figure 3D), or binned by the difference in animal density (Figure 3E), we performed two-tailed binomial tests[72] with a proposed probability of 0.5 for joining the more populated patch at each bin. The same test was used to evaluate model performance in Figure 2E.